

CASE REPORT

Identification of a novel heterozygous mutation in the *MITF* gene in an Iranian family with Waardenburg syndrome type II using next-generation sequencing

Mahzad Nasirshalal¹  | Mohammad Panahi² | Nahid Javanshir³ | Hamzeh Salmani⁴ 

¹Department of Medical Genetics, School of Medicine, Ahvaz Jundishapur University of Medical Sciences, Ahvaz, Iran

²Department of Medical Biotechnology, Faculty of Advanced Medical Sciences, Tabriz University of Medical Sciences, Tabriz, Iran

³Department of Industrial and Environmental Biotechnology, National Institute of Genetic Engineering and Biotechnology, Tabriz, Iran

⁴Department of Medical Genetics, School of Medicine, Tehran University of Medical Sciences, Tehran, Iran

Correspondence

Hamzeh Salmani, Tehran University of Medical Sciences, P.O. BOX 1416753955, Tehran, Iran.
Email: h-salmani@razi.tums.ac.ir

Funding information

The GenomeFan Company supported this research.

Abstract

Background: Waardenburg syndrome (WS) is a genetically heterogeneous syndrome with both autosomal recessive and dominant inheritance. WS causes skin and iris pigmentation accumulation and sensorineural hearing loss, in varying degrees. There are four WS types with different characteristics. WS1 and WS2 are the most common and have a dominant inheritance. WS2 is caused by mutations in the microphthalmia-associated transcription factor (*MITF*) gene.

Methods: An Iranian couple with hearing loss was recruited in the present study. First, they were screened for *GJB2* and *GJB6* gene mutations, and then whole-exome sequencing 100X was performed along with bioinformatics analysis.

Results: A novel pathogenic heterozygous mutation, c.425T>A; p.L142Ter, was detected in the *MITF* gene's exon 4. Bioinformatics analysis predicted c.425T>A; p.L142Ter as a possible pathogenic variation. It appears that the mutated transcript level declines through nonsense-mediated decay. It probably created a significantly truncated protein and lost conserved and functional domains like basic helix-loop-helix-zipper proteins. Besides, the variant was utterly co-segregated with the disease within the family.

Conclusions: We investigated an Iranian family with congenital hearing loss and identified a novel pathogenic variant c.425T>A; p. L142Ter in the *MITF* gene related to WS2. This variant is a nonsense mutation, probably leading to a premature stop codon. Our data may be beneficial in upgrading gene mutation databases and identifying WS2 causes.

KEYWORDS

MITF gene, mutation, type 2A, Waardenburg syndrome, WES

Mahzad Nasirshalal, Mohammad Panahi, Nahid Javanshir also contributed to this work equally and wrote the manuscript.

This is an open access article under the terms of the Creative Commons Attribution-NonCommercial License, which permits use, distribution and reproduction in any medium, provided the original work is properly cited and is not used for commercial purposes.

© 2021 The Authors. *Journal of Clinical Laboratory Analysis* published by Wiley Periodicals LLC.

1 | INTRODUCTION

Waardenburg syndrome (WS) is an autosomal dominantly inherited disease characterized by different degrees of sensorineural hearing loss as well as hair, skin, and eye abnormal pigmentation.^{1–3} WS affects an estimated 1 in 40,000 individuals, including two to five percent of all congenital hearing loss cases,^{4,5} and is divided into four types from WS1 to WS4. WS is caused during embryonic development with mutations in several genes in neural crest cells, which have a role in division and migration.⁶ Six genes (*PAX3*, *MITF*, *EDN3*, *EDNRB*, *SOX10*, and *SNAI2*) and two loci (*WS2B*, *WS2C*) are involved in the WS pathogenesis.⁷ WS1 and WS2 are the most common types. WS1 is caused by a mutation in the *PAX3* gene and is characterized by dystopia canthorum, while WS2 differs from the other types due to the absence of dystopia canthorum caused by mutation in the *MITF* gene. Sensorial hearing loss, progressive hearing loss, and heterochromia iridis have been reported in WS2 patients.⁸ WS3 or Waardenburg-Klein syndrome (MIM 148,820) is a more severe presentation of WS1, involving upper limb irregularities, and WS4 (MIM 277,580) presents with Hirschsprung disease; meanwhile, both have the main WS symptoms.⁹

Among the four types, WS2 is caused by a mutation in the *MITF* gene. This gene plays a crucial role in melanocyte survival and development.¹⁰ *MITF* up-regulates the expression of significant melanogenic genes such as tyrosinase (*TYR*), tyrosinase-related protein-1 (*TYRP1*), and tyrosinase-related protein-2 (*TYRP2*) by binding to the E-box motif (CANNTG) inside the promoter. These genes encode enzymes involved in the normal melanin synthesis in melanocytes.^{11,12}

Besides, WS2 is the most genetically heterogeneous; hence, for diseases with genetic heterogeneity, whole-exome sequencing (WES) technologies are useful to analyze the probable pathogenic mutation.^{13,14} Here, we conducted WES to screen all potential gene mutations associated with WS and congenital deafness and identified a novel pathogenic variant in an Iranian family with three members diagnosed with WS2.

2 | MATERIALS AND METHOD

2.1 | Clinical evaluation of proband

The proband was the third child of a non-consanguineous marriage, and he was a 31-year-old symptomatic man with congenital bilateral hearing loss and premature graying of hair. His mother was a healthy 55-year-old woman, and his father was a 63-year-old man with premature graying of hair who had died. Also, he had a brother with hearing loss, blue eyes, and premature graying of hair who has died, and a sister with premature graying of hair as well. The first molecular genetic testing for *GJB2* and *GJB6* genes was performed, and no causative genetic variant related to the patient's phenotype was detected.

2.2 | DNA extraction and quality control

The blood sample was collected from the participant for DNA extraction (with the patient's consent). DNA was extracted and purified from leukocytes with an MG blood genomic mini kit according to the manufacturer's instructions. Finally, the DNA purity and integrity were assessed using spectrophotometry (Thermo Fisher Scientific, Waltham, MA, USA) and agarose gel electrophoresis, respectively.

2.3 | Whole-exome sequencing

A total amount of 1.0 µg extracted genomic DNA was obtained from each sample. After employing the extracted genomic DNA as input material to prepare the DNA sample, it was examined using the SureSelect Human All ExonV6 kit (Agilent Technologies, CA, USA). The genomic DNA was fragmented with about 180–280 bp by the hydrodynamic shearing system (Covaris, Massachusetts, USA). Then, exonuclease/polymerase enzymes converted the remaining overhangs into blunt ends, and the enzymes were removed. Adapter oligonucleotides were ligated following adenylation of the 3' ends of DNA fragments. Selectively, DNA fragments were enriched with ligated adapter molecules on both ends in a PCR reaction. Captured libraries were enriched through a PCR reaction, which adds index tags to samples and prepares them for hybridization. Then, the AMPure XP system (Beckman Coulter, Beverly, USA) was used to purify products, and Agilent high sensitivity DNA assay on the Agilent Bioanalyzer 2100 system was used to quantify them. Finally, the captured library was sequenced on the NovaSeq 6000 Illumina sequencer with an average coverage of 100X.

2.4 | Whole-exome sequencing data analysis

For the WES data analysis, first, we evaluated the raw data quality using the FastQC and NGS QC toolkits. The quality assessment of FASTQ files showed that the number of total reads was 29,977,994 with 50% GC content. In the next step, the data were filtered by removing adapter, contaminating, and low quality reads. The resulting high-quality reads ($Q > =20$: Phred quality score above 20) were aligned to the latest human reference genome (GRCh37.p13/hg19) using the Burrows-Wheeler Alignment tool (version 0.7.17-r1188).¹⁵ After alignment, the result was stored in sequence alignment map (SAM) file format. The Picard tool (Version 2.13.2, <http://picard.sourceforge.net/>) was used to mark and remove duplicated reads and convert the SAM file to the Binary Alignment Map (BAM) format. In the next step, we performed base quality recalibration of the reads using the GATK base quality score recalibration. The variant calling step was run to investigate single-nucleotide variants and small insertions or deletions (indel) using GATK HaplotypeCaller.¹⁶ Then, false-positive variants were filtered out by GATK Variant Quality Score Recalibration.¹⁷ Parameters essential in filtering,

including variants with coverage ≥ 15 , minor allele coverage ≥ 10 , and call quality ≥ 20 , were maintained, and other variants were removed. In the final analysis step, genetic variants were annotated with the ANNOVAR tool using different databases, including dbSNP (<https://www.ncbi.nlm.nih.gov/projects/SNP>), OMIM (<https://www.omim.org>), dbNSFP (<https://sites.google.com/site/jpopgen/dbNSFP>), and population databases. Afterward, the annotated variants were filtered and prioritized according to the minor allele frequency with a cutoff value of < 0.05 in the 1000 Genomes Project, dbSNP141, Exome Aggregation Consortium (ExAC r 0.3.1), and ESP6500AA (NHLBI GO Exome Sequencing Project). Finally, the selected variants were classified according to the ACMG guideline and assigned to five categories, including pathogenic, likely pathogenic, VUS, likely benign, and benign. The OMIM database and literature were used to find the function of the variants and their correlation with the disease phenotype and inheritance pattern. The detailed analysis pipeline is schematically presented in Figure 1.

2.5 | Functional analysis of the detected mutation

The detected variant pathogenicity was evaluated using in silico software including the MutationTaster (<http://www.mutationtaster.org/>) web server. The SWISSMODEL web server (<https://swissmodel.expasy.org/>) was used (PDB 4ATI) to predict the wild-type and mutant protein structure. The I-Mutant Suite web server (<https://b2n.ir/480404>) was used to estimate the mutant protein stability compared to the typical structure through predicting $\Delta\Delta G$. The nonsense-mediated mRNA decay (NMD) ESC predictor web server was used to predict whether the detected variant would escape NMD (<https://nmdprediction.shinyapps.io/nmdescpredictor/>). Also, the STRING database and the KEGG

pathway database were used to predict the protein-protein interaction and pathway analysis, respectively.

2.6 | Validation of variants by Sanger sequencing

Sanger sequencing was performed in the proband to validate the identified pathogenic variant using WES. Primer pairs (MITF-E4-F: AAATCTTAGCCTATGAAAATCC, MITF-E4-R: CTAATGCCCTATCAAAC TGC) were designed for the candidate loci based on the reference genomic sequences of the Human Genome from GenBank in NCBI through Primer3 (bioinfo.ut.ee/primer3-0.4.0/) and PCR performed under the following conditions: initial denaturation at 95°C/4 min, followed by 30 cycles of denaturation at 95°C/30 s, annealing at 52°C/30 s, elongation at 72°C/45 s, and extension at 72°C/5 min.

3 | RESULTS

3.1 | Information of the proband

In the present study, an Iranian deaf couple attempting to conceive that was negative for *GJB2* and *GJB6* gene mutations were recruited, and WES was performed for the proband III-3 (Figure 2). The clinical information of the patient and his family is summarized in Table 1.

3.2 | Identification of the *MITF* gene variant

Following WES filtering along with in silico analysis, a novel pathogenic mutation, c. 425T>A (NM_000248: p.L142Ter) (Figures 3

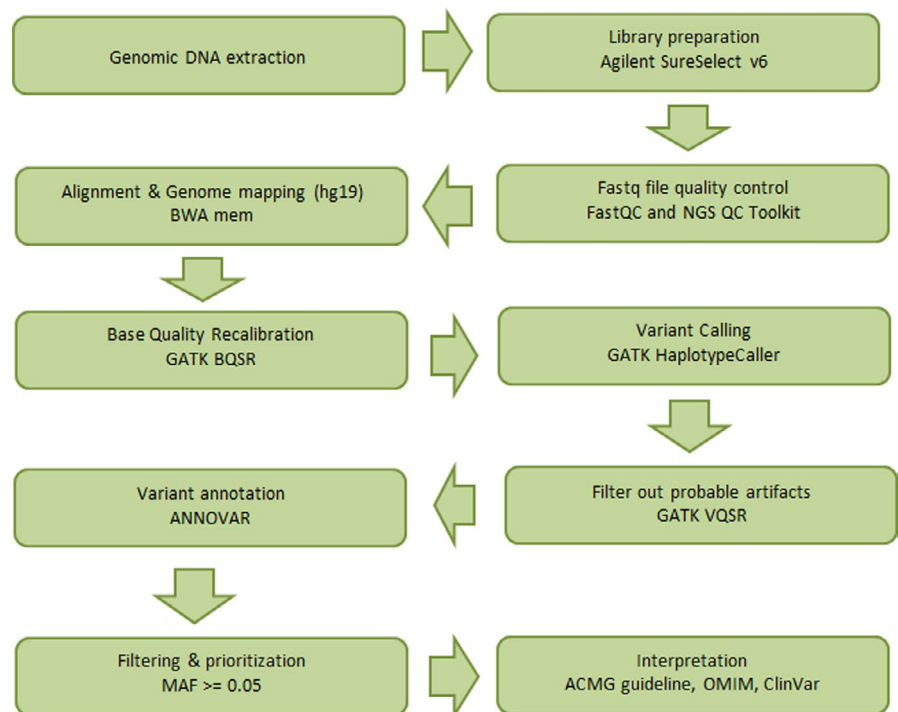


FIGURE 1 WES analysis pipeline

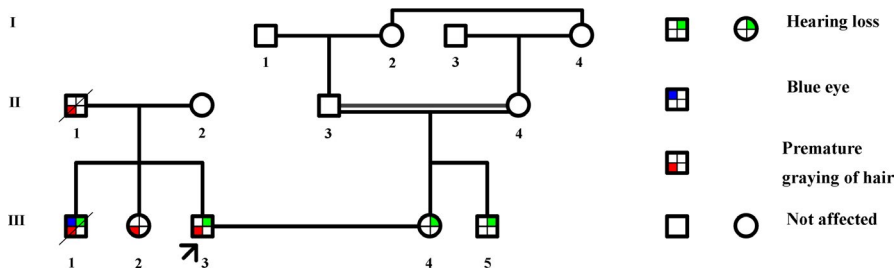


FIGURE 2 Pedigree for the Iranian family with hearing loss. Proband III-3 underwent whole-exome sequencing

Phenotype features	Proband (III-3)	Father of proband (II-1)	Sister of proband (III-2)	Brother of proband (III-1)
Age	31	63	23	NR*
Hearing loss	+	+	-	+
Degree of hearing loss	Bilateral	-	-	-
Shape of ear	Normal	Normal	Normal	Normal
Blue eye	-	+	-	+
Premature graying of hair	+	+	+	+

TABLE 1 The summary of clinical information of patient and his family

*NR; not reported.

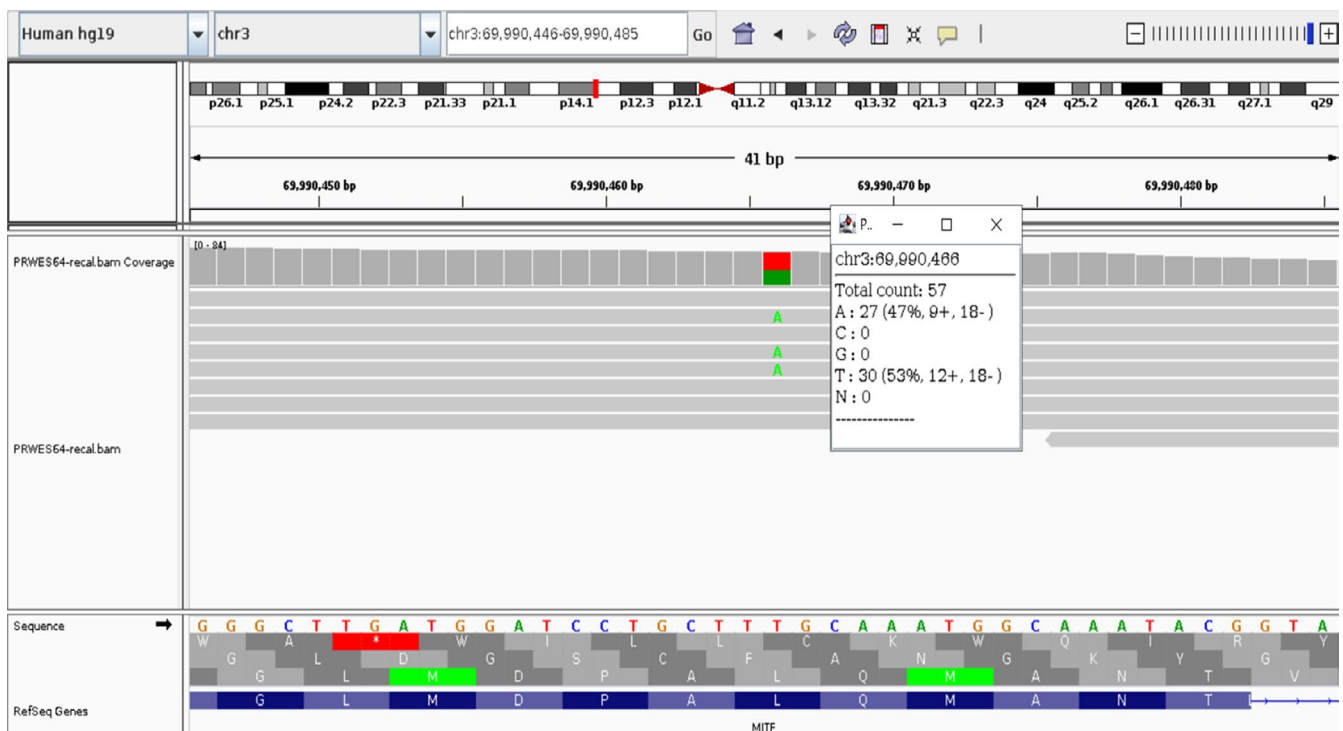


FIGURE 3 The BAM file analysis of the *MITF* gene by IGV in the proband. This illustration displays an IGV screenshot of a heterozygous substitution (c.425T>A) in exon4 of the *MITF* gene in the proband. Among the total count of 57 (nucleotide) in this position, there are 27 A as reference allele and 30 T as an alternative allele. This distribution showed that our new mutation is a heterozygous one

and 4, Table 2) was detected in the *MITF* gene's exon 4. The detected variant was confirmed by Sanger sequencing (Figure 4A). According to the ACMG classification, this variant is pathogenic and is not reported in population databases, such as ExAC, 1000

Genomes Project, and gnomAD databases, or literature on WS. Bioinformatics analysis showed that this mutation developed a premature stop-gain codon in the *MITF* gene, probably leading to loss of protein production. Moreover, in cases with premature

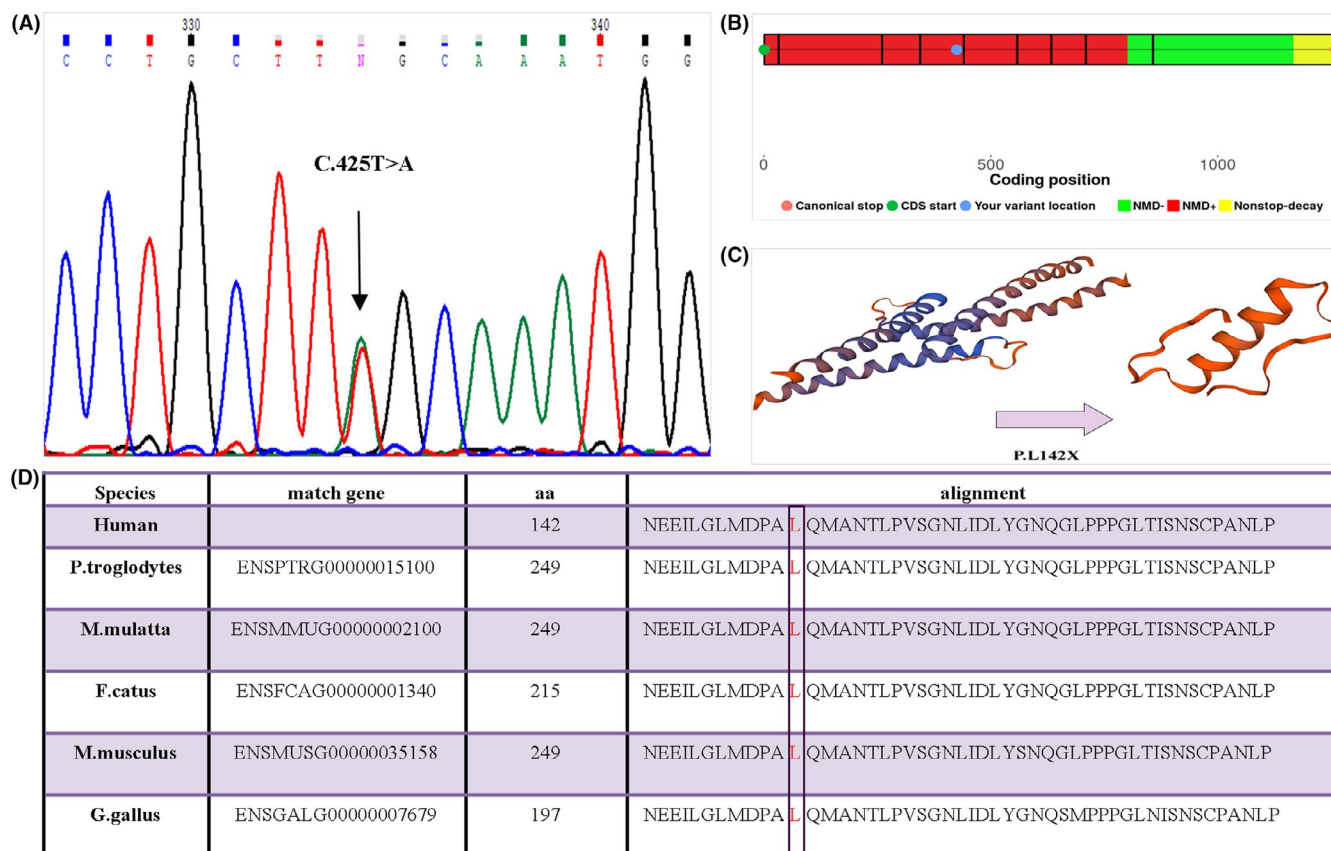


FIGURE 4 Chromatogram, position, and the possible effect of the c. 425T>A; p.L142Ter mutation in the *MITF*. (A) Confirmation of variant with Sanger sequencing, (B) the result of nonsense-mediated mRNA decay prediction in patient 1 by the NMD Esc Predictor Web site, (C) Prediction the effect of P. L142Ter mutation on the protein structure and chains using Swiss model. (D) Multi-species conservative analysis of *MITF* showing the highly conserved L142 residue (pointed by the arrow)

TABLE 2 Prediction the effect of the detected variation using MutationTaster

Analyzed issue	Analyzed results
Summary	NMD amino acid sequence changed protein features (might be) affected
Alteration (Phys/location)	chr3:69990466T>A
Ensembl transcript ID	ENST00000394351
GenBank transcript ID	NM_000248
DNA changes	c.425T>A cDNA.545T>A g.201881T>A
AA changes	L142Ter
Prediction	Disease causing
Alteration type	single base exchange
PhastCons ^a	0.93
PhyloP ^b	0.445

^aThe closer the value is to 1; the more probable the nucleotide is conserved.

^bThe closer the value is to 0; the more probable the nucleotide is conserved.

mRNA escaping from NMD, the produced protein appeared to be truncated to 142 amino acids. The SWISSMODEL web server showed that this mutation caused a loss of conserved domain like bHLHZip (Figures 4C and 5A). Moreover, the NMD prediction web server showed that this premature stop codon likely caused NMD

(Figure 4B). The $\Delta\Delta G$ value was predicted about -2.39 kcal/mol using I-Mutant with the reliability index of 9, explaining a large decrease in stability for the mutant protein structure. The segregation analysis showed that II-1 and III-1 (Figure 2) were heterozygote for this variation.

3.3 | Functional annotation of the *MITF* protein

MITF is a 58,795 Da protein with 526aa (Figure 5A). The *MITF* functional annotation by DAVID showed that this protein was expressed in most human tissues. It mainly has high quantities in the uterus, retina, pineal gland, and adipocytes according to the (<http://biogps.org>). The *MITF* protein has also been detected in different diseases like WS2A, Tietz albinism-deafness syndrome, melanoma, cutaneous malignant 8, coloboma, osteoporosis, microphthalmia, macrocephaly, albinism, and deafness. Based on InterProScan as a protein domain analysis tool, *MITF* encodes a transcription factor containing both a helix-loop-helix structure and a leucine zipper. Protein-protein interaction analysis by STRING showed that *MITF* created a network with about ten different gene products (Figure 5C). Moreover, according to the KEGG database result, this protein plays a role in six different pathways with melanogenesis being among the most important ones (Figure 5B).

4 | DISCUSSION

WS is a clinically and genetically heterogeneous disorder. Thus far, it has been documented that WS has four subtypes, and many genes have been associated with them. In this regard, *MITF* is the WS2A-associated gene characterized by sensorineural hearing loss and depigmentation spots, which might occur with or without ocular albinism. These characteristics can demonstrate variable expression and incomplete penetrance.¹⁸ WS type II (WS2; OMIM:193510) is the most common type of WS in many populations, inherited with an autosomal dominant pattern.¹⁹ Also, WS2 has familial and sporadic types with a wide variety of phenotypes that allow the study of parentage to discern the relationship between genotypes and phenotypes.²⁰

Moreover, despite several attempts to clinically distinguish between WS subtypes through diagnostic criteria, the unusual and highly varied expression has restricted the ability to make an adequate diagnosis in individual patients.¹³ In general populations,

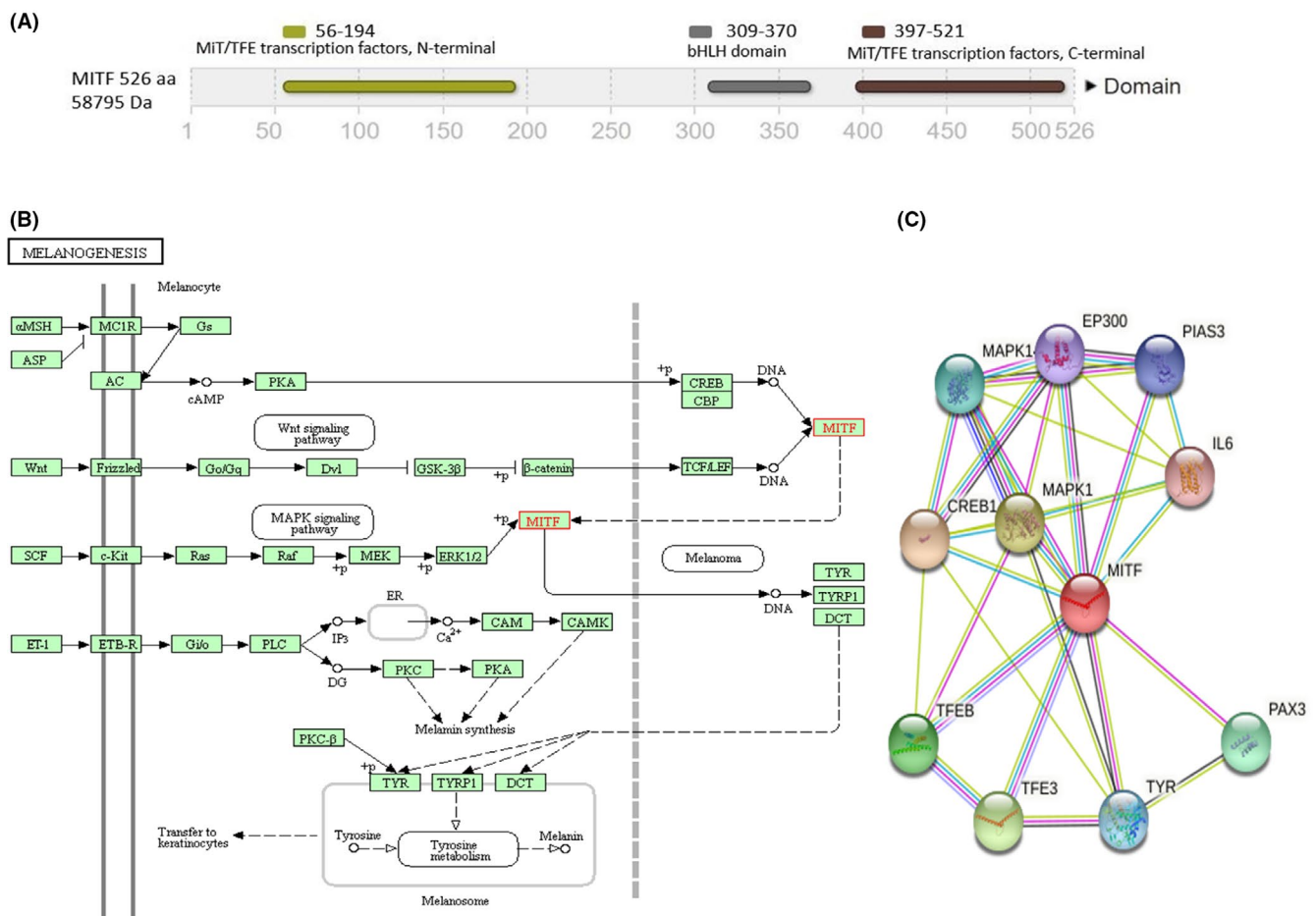


FIGURE 5 Schematic illustration of *MITF*, its pathway, and network. (A) *MITF* gene encodes a protein (58,795 Da; 526 amino acid) with three domains (MiT/TFE_N, bHLH_dom, MiT/TFE_C) (B) *MITF* as a transcription factor activates the transcription of tyrosinase and tyrosinase-related protein 1 (TYRP1), and dopachrome tautomerase (DCT). These enzymes are expressed explicitly in the melanocyte. The DCT promoter regulation involves other proteins like CREB and SOX10; and PAX3 that have an inhibitory effect on DCT activation by *MITF*. The *MITF* promoter is also partially regulated by specific transcription factors such as SOX10, PAX3, LEF-1/TCF, and CREB during development. Mutations of the *MITF* gene can lead to pigmentary and auditory defects. (C) Protein-protein interaction network of *MITF*

hearing loss and early graying are relatively normal and are not specific to WS.¹⁴ Accordingly, identifying WS genetic causes should be considered an appropriate diagnosis of WS. In this regard, more than 70 *MITF* gene mutations have been reported related to WS2A (<http://www.hgmd.cf.ac.uk/ac/index.php>). However, some patients have been found to carry none of these common variants. With the development of next-generation sequencing, new single-gene causes are observed to be responsible for WS in some cases. Moreover, although several mutations have been known to be associated with WS2 in many populations, they have rarely been investigated in the Iranian population, with only two records published on *MITF* gene mutations. The p.R293Ter variation as a novel and pathogenic mutation, located in exon 9, and p.R214Ter as a de novo heterozygous variant and recurrent *MITF* variant in exon 7 are related to WS2. Herein, we found another novel pathogenic variant, called c.425T>A (p. L142Ter), in the *MITF* gene's exon 4. Therefore, our candidate variation is the third reported *MITF*-associated variation correlated with WS2 in the Iranian population.

This study surveyed a pedigree with different degrees of hearing loss in the family members. III-4 and III-5 both had congenital moderate hearing loss, III1 had profound congenital deafness, and III-3 had congenital bilateral hearing loss. Genetics analysis showed that all the cases had the c.425T>A; p. L142Ter variant occurring with the heterozygous state in the *MITF* gene. This pathogenic variant was novel and was located in a conserved sequence of the *MITF* gene's exon 4, subsequently producing premature mRNA. The *MITF* gene encompasses nine isoforms, all of which have exons 2–9 in common and encode the functional domain of the transcription factor. In this regard, the BHLH domain is encoded by exons 6, 7, and 8.²¹ It has been shown that mRNA shorter than a specified length is almost entirely degraded. This mechanism is known as nonsense-mediated mRNA decay (NMD).²² Hence, mRNA containing a premature termination codon (PTC) is probably degraded through NMD. As for this, NMD is induced if a PTC is placed more than 50–55 nucleotides upstream of the exon-exon junction and degrades mRNA.²³ Hence, NMD causes loss-of-function alleles.²⁴ Regarding the detected variant in this report, NMD appears to have high possibility because the variant was discovered early in a long-distance transcript, more than 300 bp upstream of the last exon-exon junction in the mRNA transcript. Nevertheless, in cases that premature mRNA escapes from NMD, the produced protein appears to be truncated to 142 amino acids instead of the wild-type protein with 442 residues. As a result, the disease can occur due to the gain-of-function effects because the truncated protein loses conserved and functional domains like bHLHZip. The bHLHZip domain is found in *MITF*. The bHLHZip subfamily carries a C-terminal leucine zipper, which significantly lengthens the helix 2 α -helix of HLH. These proteins attach DNA as the TFE3 homo- or heterodimers with the relevant proteins TFEB and TFEC.²⁵ The *MITF* gene, identified as the Class E basic helix-loop-helix protein 32, is a bHLHZip transcription factor included in neural crest melanocyte development and the pigmented retinal epithelium. It controls genes' expressions that are important in cell differentiation,

survival, and proliferation. It connects to M-boxes (5'-TCATGTG-3') and E-boxes (5'-CACGTG-3') located in target gene promoters, including *BCL2* and *TYR*. The *MITF* gene works through tyrosinase to control melanin production and is also directly involved in the molecular hearing process.²⁶ Therefore, we deduced the probability of defective tyrosinase transactivation due to the c.425T>A variation that deleted *MITF* recognition sequences within *TYR*'s promoter sequence. Hence, such a truncated protein disrupts the *MITF* gene function and ending in the WS2A phenotype.

We investigated the clinical and genetic characteristics of an Iranian family with WS2A in a pedigree of an autosomal dominant WS. We identified a novel pathogenic variant, c.425T>A; p. L142Ter, in the *MITF* gene. The variant was completely co-segregated with the disease phenotype, and all the patients were heterozygote for the variant. This variant produced a premature stop codon, which is likely to degrade the transcript through the NMD pathway. However, more findings are required to confirm the pathogenicity of the detected variant.

ACKNOWLEDGMENTS

The authors are thankful to Dr. Hamzeh Rahimi and the GenomeFan Company for supporting this project.

CONFLICT OF INTEREST

The authors declare no conflicts of interest.

AUTHOR CONTRIBUTIONS

Mahzad Nasirshalal, Mohammad Panahi, and Nahid Javanshir contributed to WES filtering, bioinformatics analysis, data interpretation regarding the whole-exome sequencing and WS type II. These authors also contributed to this work equally and wrote the manuscript. HS supervised, reviewed, and edited the manuscript. All the authors read and approved the final manuscript.

DATA AVAILABILITY STATEMENT

The data supporting this study's findings are available from the corresponding author upon reasonable request.

ORCID

Mahzad Nasirshalal  <https://orcid.org/0000-0002-6097-3168>

Hamzeh Salmani  <https://orcid.org/0000-0001-9982-0807>

REFERENCES

- Hoth CF, Milunsky A, Lipsky N, Sheffer R, Clarren SK, Baldwin CT. Mutations in the paired domain of the human PAX3 gene cause Klein-Waardenburg syndrome (WS-III) as well as Waardenburg syndrome type I (WS-I). *Am J Hum Genet.* 1993;52(3):455-462.
- Yang T, Li X, Huang Q, et al. Double heterozygous mutations of *MITF* and *PAX3* result in Waardenburg syndrome with increased penetrance in pigmentary defects. *Clin Genet.* 2013;83(1):78-82.
- Zaman A, Capper R, Baddoo W. Waardenburg syndrome: more common than you think!. *Clin Otolaryngol.* 2015;40(1):44-48.
- Christopher M. AMLS. 乳鼠心肌提取 HHS public access. *Physiol Behav.* 2016;176(1):100-106.
- Scheerer NE, Jones JA. The role of auditory feedback at vocalization onset and mid-utterance. *Front Psychol.* 2018;9(October):1-9.

6. Pingault V, Ente D, Dastot-Le Moal F, Goossens M, Marlin S, Bondurand N. Review and update of mutations causing Waardenburg syndrome. *Hum Mutat*. 2010;31(4):391-406.
7. Song J, Feng Y, Acke FR, Coucke P, Vleminckx K, Dhooge IJ. Hearing loss in Waardenburg syndrome: a systematic review. *Clin Genet*. 2016;89(4):416-425.
8. Saberi M, Golchehre Z, Salmani H, Karamzade A. First report of Klein-Waardenburg Syndrome in Iran and a novel pathogenic splice site variant in PAX3 gene. *Int J Pediatr Otorhinolaryngol*. 2018;113(August):229-233. <https://doi.org/10.1016/j.ijporl.2018.08.009>
9. Barashkov NA, Romanov GP, Borisova UP, Solovyev AV. A rare case of Waardenburg syndrome with unilateral hearing loss caused by nonsense variant c. 772C > T (p. Arg259 *) in the MITF gene in Yakut patient from the Eastern Siberia (Sakha Republic, Russia). *Int J Circumpolar Health*. 2019;78(1):4-7. <https://doi.org/10.1080/22423982.2019.1630219>
10. Zhang H, Luo H, Chen H, et al. Functional analysis of MITF gene mutations associated with Waardenburg syndrome type 2. *FEBS Lett*. 2012;586(23):4126-4131. <https://doi.org/10.1016/j.febsl.2012.10.006>
11. Ni C, Zhang D, Beyer LA, et al. Hearing dysfunction in heterozygous Mitf^{Mi-wh/+} mice, a model for Waardenburg syndrome type 2 and Tietz syndrome. *Pigment Cell Melanoma Res*. 2013;26(1):78-87.
12. Cheli Y, Ohanna M, Ballotti R, Bertolotto C. Fifteen-year quest for microphthalmia-associated transcription factor target genes. *Pigment Cell Melanoma Res*. 2010;23(1):27-40.
13. Ren S, Chen X, Kong X, et al. Identification of six novel variants in Waardenburg syndrome type II by next-generation sequencing. *Mol Genet Genomic Med*. 2020;8(3):1-11.
14. Jang MA, Lee T, Lee J, Cho EH, Ki CS. Identification of a novel de novo variant in the PAX3 gene in Waardenburg syndrome by diagnostic exome sequencing: the first molecular diagnosis in Korea. *Ann Lab Med*. 2015;35(3):362-365.
15. Han P, Wei G, Cai K, et al. Identification and functional characterization of mutations in LPL gene causing severe hypertriglyceridaemia and acute pancreatitis. *J Cell Mol Med*. 2020;24(2):1286-1299.
16. Zheng Y, Xu J, Liang S, Lin D, Banerjee S. Whole exome sequencing identified a novel heterozygous mutation in HMBS gene in a Chinese patient with acute intermittent porphyria with rare type of mild anemia. *Front Genet*. 2018;9(April):1-5.
17. Zhang R, Chen S, Han P, et al. Whole exome sequencing identified a homozygous novel variant in CEP290 gene causes Meckel syndrome. *J Cell Mol Med*. 2020;24(2):1906-1916.
18. Pang X, Zheng X, Kong X, et al. A homozygous MITF mutation leads to familial Waardenburg syndrome type 4. *Am J Med Genet Part A*. 2019;179(2):243-248.
19. Jalilian N, Tabatabaiefar MA, Yazdanpanah M, et al. A comprehensive genetic and clinical evaluation of Waardenburg syndrome type II in a set of Iranian patients. *Int J Mol Cell Med*. 2018;7(1):17.
20. Yan X, Zhang T, Wang Z, et al. A novel mutation in the MITF may be digenic with GJB2 mutations in a large Chinese family of Waardenburg syndrome type II. *J Genet Genomics*. 2011;38(12):585-591. <https://doi.org/10.1016/j.jgg.2011.11.003>
21. Levy C, Khaled M, Fisher DE. MITF: master regulator of melanocyte development and melanoma oncogene. *Trends Mol Med*. 2006;12(9):406-414.
22. Kim WK, Yun S, Kwon Y, et al. MRNAs containing NMD-competent premature termination codons are stabilized and translated under UPF1 depletion. *Sci Rep*. 2017;7(1):1-13. <https://doi.org/10.1038/s41598-017-16177-9>
23. Kurosaki T, Popp MW, Maquat LE, Popp MW. Mediated mRNA decay. *Nat Rev Mol Cell Biol*. 2019;20(7):406-420.
24. Coban-Akdemir Z, White JJ, Song X, et al. Identifying genes whose mutant transcripts cause dominant disease traits by potential gain-of-function alleles. *Am J Hum Genet*. 2018;103(2):171-187. <https://doi.org/10.1016/j.ajhg.2018.06.009>
25. Takeda K, Takemoto C, Kobayashi I, et al. Ser298 of MITF, a mutation site in Waardenburg syndrome type 2, is a phosphorylation site with functional significance. *Hum Mol Genet*. 2000;9(1):125-132.
26. Thongpradit S, Jinawath N, Javed A, Noojarern S. OPEN MITF variants cause nonsyndromic sensorineural hearing loss with autosomal recessive inheritance. *Sci Rep*. 2020;10(1):1-11.

How to cite this article: Nasirshalal M, Panahi M, Javanshir N, Salmani H. Identification of a novel heterozygous mutation in the MITF gene in an Iranian family with Waardenburg syndrome type II using next-generation sequencing. *J Clin Lab Anal*. 2021;35:e23792. <https://doi.org/10.1002/jcla.23792>